

Properties of β -stable neutron star matter with hyperons

I. Vidaña, A. Polls, and A. Ramos

Departament d'Estructura i Constituents de la Matèria, Universitat de Barcelona, E-08028

Barcelona, Spain

Ø. Elgarøy, L. Engvik, and M. Hjorth-Jensen

Department of Physics, University of Oslo, N-0316 Oslo, Norway

Abstract

We present results from many-body calculations for β -stable neutron star matter with nucleonic and hyperonic degrees of freedom, employing the most recent parametrizations of the baryon-baryon interaction of the Nijmegen group. It is found that the only strange baryons emerging in β -stable matter up to total baryonic densities of 1.2 fm^{-3} are Σ^- and Λ . The corresponding equations of state are thence used to compute properties of neutron stars such as the masses, moments of inertia and radii. We also study the possibility of forming a hyperon superfluid and discuss its implications for neutron stars.

PACS numbers: 13.75.Ev, 21.30.-x, 21.65.+f, 26.60.+c, 97.60.Gb, 97.60.Jd

Typeset using REVTeX

I. INTRODUCTION

The physics of compact objects like neutron stars offers an intriguing interplay between nuclear processes and astrophysical observables. Neutron stars exhibit conditions far from those encountered on earth; typically, expected densities ρ of a neutron star interior are of the order of 10^3 or more times the density $\rho_d \approx 4 \cdot 10^{11}$ g/cm³ at 'neutron drip', the density at which nuclei begin to dissolve and merge together. Thus, the determination of an equation of state (EoS) for dense matter is essential to calculations of neutron star properties. The EoS determines properties such as the mass range, the mass-radius relationship, the crust thickness and the cooling rate. The same EoS is also crucial in calculating the energy released in a supernova explosion.

At densities near to the saturation density of nuclear matter, (with number density $n_0 = 0.16$ fm⁻³), we expect the matter to be composed of mainly neutrons, protons and electrons in β -equilibrium, since neutrinos have on average a mean free path larger than the radius of the neutron star. The equilibrium conditions can then be summarized as

$$\mu_n = \mu_p + \mu_e, \quad n_p = n_e, \quad (1)$$

where μ_i and n_i refer to the chemical potential and number density in fm⁻³ of particle species i , respectively. At the saturation density of nuclear matter, n_0 , the electron chemical potential is of the order ~ 100 MeV. Once the rest mass of the muon is exceeded, it becomes energetically favorable for an electron at the top of the e^- Fermi surface to decay into a μ^- . We then develop a Fermi sea of degenerate negative muons, and we have to modify the charge balance according to $n_p = n_e + n_\mu$, and require that $\mu_e = \mu_\mu$.

As the density increases, new hadronic degrees of freedom may appear in addition to neutrons and protons. One such degree of freedom is hyperons, baryons with a strangeness content. Contrary to terrestrial conditions where hyperons are unstable and decay into nucleons through the weak interaction, the equilibrium conditions in neutron stars can make the inverse process happen, so that the formation of hyperons becomes energetically favorable. As soon as the chemical potential of the neutron becomes sufficiently large, energetic

neutrons can decay via weak strangeness non-conserving interactions into Λ hyperons leading to a Λ Fermi sea with $\mu_\Lambda = \mu_n$. However, one expects Σ^- to appear via

$$e^- + n \rightarrow \Sigma^- + \nu_e, \quad (2)$$

at lower densities than the Λ , even though Σ^- is more massive. The negatively charged hyperons appear in the ground state of matter when their masses equal $\mu_e + \mu_n$, while the neutral hyperon Λ appears when μ_n equals its mass. Since the electron chemical potential in matter is larger than the mass difference $m_{\Sigma^-} - m_\Lambda = 81.76$ MeV, Σ^- will appear at lower densities than Λ . For matter with hyperons as well the chemical equilibrium condition becomes,

$$\begin{aligned} \mu_{\Xi^-} &= \mu_{\Sigma^-} = \mu_n + \mu_e, \\ \mu_\Lambda &= \mu_{\Xi^0} = \mu_{\Sigma^0} = \mu_n, \\ \mu_{\Sigma^+} &= \mu_p = \mu_n - \mu_e. \end{aligned} \quad (3)$$

We have omitted isobars Δ , see the discussion below.

Hyperonic degrees of freedom have been considered by several authors, but mainly within the framework of relativistic mean field models [1–3] or parametrized effective interactions [4], see also Balberg *et al.* [5] for a recent update. Realistic hyperon-nucleon interactions were employed by Schulze *et al.* recently, see Ref. [6], in a many-body calculation in order to study where hyperons appear in neutron star matter. All these works show that hyperons appear at densities of the order of $\sim 2n_0$.

In Ref. [6] however, one was only able to fix the density where Σ^- appears, since only a hyperon-nucleon interaction was employed. As soon as Σ^- appears, one needs a hyperon-hyperon interaction in order to estimate e.g., the self-energy of Λ . The aim of this work is thus to present results from many-body calculations of hyperonic degrees of freedom for β -stable neutron star matter employing interactions which also account for strangeness $S < -1$. To achieve this goal, our many-body scheme starts with the most recent parametrization of the free baryon-baryon potentials for the complete baryon octet

as defined by Stoks and Rijken in Ref. [7]. This entails a microscopic description of matter starting from realistic nucleon-nucleon, hyperon-nucleon and hyperon-hyperon interactions. In a recent work [8] we have developed a formalism for microscopic Brueckner-type calculations of dense nuclear matter that includes all types of baryon-baryon interactions and allows to treat any asymmetry on the fractions of the different species ($n, p, \Lambda, \Sigma^-, \Sigma^0, \Sigma^+, \Xi^-$ and Ξ^0). Results for various fractions of the above particles were also discussed.

Here we extend the calculations of Ref. [8] to studies of β -stable neutron star matter. Our results, together with a brief summary of the formalism discussed in Ref. [8], are presented in section II. There we discuss the equation of state (EoS) and the composition of β -stable matter with various baryon-baryon potentials. Based on the composition of matter we present also results for baryon superfluidity and discuss the possible neutron star structures.

II. EQUATION OF STATE AND COMPOSITION OF β -STABLE MATTER

Our many-body scheme starts with the most recent parametrization of the free baryon-baryon potentials for the complete baryon octet as defined by Stoks and Rijken in Ref. [7]. This potential model, which aims at describing all interaction channels with strangeness from $S = 0$ to $S = -4$, is based on $SU(3)$ extensions of the Nijmegen potential models [9] for the $S = 0$ and $S = -1$ channels, which are fitted to the available body of experimental data and constrain all free parameters in the model. In our discussion we employ the interaction version NSC97e of Ref. [7], since this model, together with the model NSC97f of Ref. [7], result in the best predictions for hypernuclear observables [9]. For a discussion of other interaction models, see Refs. [7,10].

A. Formalism

With a given interaction model, the next step is to introduce effects from the nuclear medium. Here we will construct the so-called G -matrix, which takes into account short-range correlations for all strangeness sectors, and solve the equations for the single-particle

energies of the various baryons self-consistently. The G -matrix is formally given by

$$\begin{aligned} \langle B_1 B_2 | G(\omega) | B_3 B_4 \rangle &= \langle B_1 B_2 | V | B_3 B_4 \rangle + \\ &\sum_{B_5 B_6} \langle B_1 B_2 | V | B_5 B_6 \rangle \frac{1}{\omega - \varepsilon_{B_5} - \varepsilon_{B_6} + i\eta} \\ &\times \langle B_5 B_6 | G(\omega) | B_3 B_4 \rangle. \end{aligned} \quad (4)$$

Here B_i represents all possible baryons n , p , Λ , Σ^- , Σ^0 , Σ^+ , Ξ^- and Ξ^0 and their quantum numbers such as spin, isospin, strangeness, linear momenta and orbital momenta. The intermediate states $B_5 B_6$ are those which are allowed by the Pauli principle, and the energy variable ω is the starting energy defined by the single-particle energies of the incoming external particles $B_3 B_4$. The G -matrix is solved using relative and centre-of-mass coordinates, see e.g., Refs. [8,10] for computational details. The single-particle energies are given by

$$\varepsilon_{B_i} = t_{B_i} + u_{B_i} + m_{B_i} \quad (5)$$

where t_{B_i} is the kinetic energy and m_{B_i} the mass of baryon B_i . The single-particle potential u_{B_i} is defined by

$$u_{B_i} = \text{Re} \sum_{B_j \leq F_j} \langle B_i B_j | G(\omega = \varepsilon_{B_i} + \varepsilon_{B_j}) | B_i B_j \rangle. \quad (6)$$

The linear momentum of the intermediate single-particle state B_j is limited by the size of the Fermi surface F_j for particle species B_j . The last equation is displayed in terms of Goldstone diagrams in Fig. 1. Diagram (a) represents contributions from nucleons only as hole states, while diagram (b) has only hyperons as holes states in case we have a finite hyperon fraction in β -stable neutron star matter. The external legs represent nucleons and hyperons.

The total non-relativistic energy density, ε , and the total binding energy per baryon, \mathcal{E} , can be evaluated from the baryon single-particle potentials in the following way

$$\varepsilon = 2 \sum_B \int_0^{k_F^{(B)}} \frac{d^3 k}{(2\pi)^3} \left(\frac{\hbar^2 k^2}{2M_B} + \frac{1}{2} U_B(k) \right) \quad (7)$$

$$\mathcal{E} = \frac{\varepsilon}{n}, \quad (8)$$

where n is the total baryonic density. The density of a given baryon species is given by

$$n_B = \frac{k_{FB}^3}{3\pi^2} = x_B n , \quad (9)$$

where $x_B = n_B/n$ is the fraction of baryon B , which is of course constrained by

$$\sum_B x_B = 1 . \quad (10)$$

Detailed expressions for the single-particle energies and the G -matrices involved can be found in Ref. [8]. In order to satisfy the equations for β -stable matter summarized in Eq. (3), we need to solve Eqs. (4) and (5) to obtain the single-particle energies of the particles involved at the corresponding Fermi momenta. Typically, for every total baryonic density $n = n_N + n_Y$, the density of nucleons plus hyperons, Eqs. (4) and (5) were solved for five nucleon fractions and five hyperons fractions and, for every nucleon and hyperon fraction, we computed three proton fractions and three fractions for the relevant hyperons. The set of equations in Eq. (3) were then solved by interpolating between different nucleon and hyperon fractions.

The many-body approach outlined above is the lowest-order Brueckner-Hartree-Fock (BHF) method extended to the hyperon sector. This means also that we consider only two-body interactions. However, it is well-known from studies of nuclear matter and neutron star matter with nucleonic degrees of freedom only that three-body forces are important in order to reproduce the saturation properties of nuclear matter, see e.g., Ref. [11] for the most recent approach. In order to include such effects, we replace the contributions to the proton and neutron self-energies arising from intermediate nucleonic states only, see diagram (a) of Fig. 1, with those derived from Ref. [11] (hereafter APR98) where the Argonne V_{18} nucleon-nucleon interaction [12] is used with relativistic boost corrections and a fitted three-body interaction, model. The calculations of Ref. [11] represent at present perhaps the most sophisticated many-body approach to dense matter. In the discussions below we will thus present two sets of results for β -stable matter, one where the nucleonic contributions to the self-energy of nucleons is derived from the baryon-baryon potential model of Stoks

and Rijken [7] and one where the nucleonic contributions are replaced with the results from Ref. [11] following the parametrization discussed in Eq. (49) of Ref. [13]. Replacing the nucleon-nucleon part of the interaction model of Ref. [7] with that from the V_{18} nucleon-nucleon interaction [12], does not introduce large differences at the BHF level. However, the inclusion of three-body forces as done in Ref. [11] is important. Hyperonic contributions will however all be calculated with the baryon-baryon interaction of Stoks and Rijken [7].

B. β -stable neutron star matter

The above models for the pure nucleonic part combined with the hyperon contribution yield the composition of β -stable matter, up to total baryonic number density $n = 1.2 \text{ fm}^{-3}$, shown in Fig. 2. The corresponding energies per baryon are shown in Fig. 3 for both pure nucleonic (BHF and APR98 pn-matter) and hyperonic matter (BHF and APR98 with hyperons) in β -equilibrium for the same baryonic densities as in Fig. 2.

For both types of calculations Σ^- appears at densities $\sim 2 - 3n_0$. Since the EoS of APR98 for nucleonic matter yields a stiffer EoS than the corresponding BHF calculation, Σ^- appears at $n = 0.27 \text{ fm}^{-3}$ for the APR98 EoS and $n = 0.35 \text{ fm}^{-3}$ for the BHF EoS. These results are in fair agreement with results obtained from mean field calculations, see e.g., Refs. [1–3]. The introduction of hyperons leads to a considerable softening of the EoS. Moreover, as soon as hyperons appear, the leptons tend to disappear, totally in the APR98 case whereas in the BHF calculation only muons disappear. For the APR98 case, positrons appear at higher densities, i.e., $n = 1.18 \text{ fm}^{-3}$. This result is related to the fact that Λ does not appear at the densities considered here for the BHF EoS. For the APR98 EoS, Λ appears at a density $n = 0.67 \text{ fm}^{-3}$. Recalling $\mu_\Lambda = \mu_n = \mu_p + \mu_e$ and that the APR98 EoS is stiffer due to the inclusion of three-body forces, this clearly enhances the possibility of creating a Λ with the APR98 EoS. However, the fact that Λ does not appear in the BHF calculation can also, in addition to the softer EoS, be retraced to a delicate balance between the nucleonic and hyperonic hole state contributions (and thereby to features of the baryon-

baryon interaction) to the self-energy of the baryons considered here, see diagrams (a) and (b) in Fig. 1. Stated differently, the contributions from Σ^- , proton and neutron hole states to the Λ chemical potential are not attractive enough to lower the chemical potential of the Λ so that it equals that of the neutron. Furthermore, the chemical potential of the neutron does not increase enough since contributions from Σ^- hole states to the neutron self-energy are attractive, see e.g., Ref. [8] for a detailed account of these aspects of the interaction model.

We illustrate the role played by the two different choices for nucleonic EoS in Fig. 4 in terms of the chemical potentials for various baryons for matter in β -equilibrium. We also note that, using the criteria in Eq. (3), neither the Σ^0 nor Σ^+ do appear for both the BHF and the APR98 equations of state. This is due to the fact that none of the Σ^0 -baryon and Σ^+ -baryon interactions are attractive enough. A similar argument applies to Ξ^0 and Ξ^- . In the latter case the mass of the particle is ~ 1315 MeV and almost 200 MeV in attraction is needed in order to fulfill e.g., the condition $\mu_\Lambda = \mu_{\Xi^0} = \mu_n$. This has also been checked by us [14] in studies of the self-energy of Ξ^- in finite nuclei, using the recipe outlined in Ref. [15]. For both light and medium heavy nuclei, Ξ^- is unbound with the present hyperon-hyperon interactions, except for version NSC97f of Ref. [7]. The latter results in a weakly bound Ξ^- , in agreement with the recent studies of Batty *et al.* [16]. From the bottom panel of Fig. 4 we see however that Σ^0 could appear at densities close to 1.2 fm^{-3} . Thus, for the present densities, which would be within the range of energies for where the interaction model has been fitted, the only hyperons which can appear are Σ^- and Λ .

In summary, using the realistic EoS of Akmal *et al.* [11] for the nucleonic sector and including hyperons through the most recent model for the baryon-baryon interaction of the Nijmegen group [7], we find through a many-body calculation for matter in β -equilibrium that Σ^- appears at a density of $n = 0.27 \text{ fm}^{-3}$ while Λ appears at $n = 0.67 \text{ fm}^{-3}$. Due to the formation of hyperons, the matter is de-leptonized at a density of $n = 0.85 \text{ fm}^{-3}$. Within our many-body approach, no other hyperons appear at densities below $n = 1.2 \text{ fm}^{-3}$. Although the EoS of Akmal *et al.* [11] may be viewed as the currently most realistic approach to the

nucleonic EoS, our results have to be gauged with the uncertainty in the hyperon-hyperon and nucleon-hyperon interactions. Especially, if the hyperon-hyperon interactions tend to be more attractive, this may lead to the formation of hyperons such as the Λ , Σ^0 , Σ^+ , Ξ^- and Ξ^0 at lower densities. The hyperon-hyperon interaction and the stiffness of the nucleonic contribution play crucial roles in the formation of various hyperons. These results differ from present mean field calculations [1–3], where all kinds of hyperons can appear at the densities considered here.

C. Baryon superfluidity in β -stable matter

A generic feature of fermion systems with attractive interactions is that they may be superfluid in a region of the density-temperature plane. The 1S_0 wave of the nucleon-nucleon interaction is the best known and most investigated case in neutron stars, and the results indicate that one may expect a neutron superfluid in the inner crust of the star and a proton superfluid in the quantum liquid interior, both with energy gaps of the order of 1 MeV [17–22]. Furthermore, neutrons in the quantum liquid interior may form a superfluid due to the attractive 3P_2 - 3F_2 wave of the nucleon-nucleon interaction [23]. Baryon superfluidity has important consequences for a number of neutron star phenomena, including glitches [24] and cooling [25]. If hyperons appear in neutron stars, they may also form superfluids if their interactions are sufficiently attractive. The case of Λ superfluidity has been investigated by Balberg and Barnea [26] using parametrized effective Λ - Λ interactions. Results for Λ and Σ^- -pairing using bare hyperon-hyperon interaction models have recently been presented by Takatsuka and Tamagaki [27]. The result of both groups indicate the presence of a Λ superfluid for baryon densities in the range of 2 – $4n_0$. The latter authors also suggest that the formation of a Σ^- superfluid may be more likely than Λ -superfluidity. Along the lines followed by these authors we will here present results for hyperon superfluidity within our model.

The crucial quantity in determining the onset of superfluidity is the energy gap function

$\Delta(\mathbf{k})$. The value of this function at the Fermi surface is proportional to the critical temperature of the superfluid, and by determining Δ we therefore map out the region of the density-temperature plane where the superfluid may exist. When the 1S_0 interaction is the driving cause of the superfluidity, the gap function becomes isotropic and depends on the magnitude of \mathbf{k} only. It can be determined by solving the BCS gap equation

$$\Delta(k) = -\frac{1}{\pi} \int_0^\infty dk' k'^2 \tilde{V}_{1S_0}(k, k') \frac{\Delta(k')}{\sqrt{(\epsilon_{k'} - \mu)^2 + \Delta(k')^2}}, \quad (11)$$

In this equation, ϵ_k is the momentum-dependent single particle energy in the medium for the particle species in question, μ is the corresponding chemical potential, and \tilde{V}_{1S_0} is the effective pairing interaction. At this point we emphasize that using parametrized effective interactions in the gap equation can lead to errors. The gap equation includes diagrams also found in the G -matrix, and one therefore needs to calculate \tilde{V} systematically from microscopic many-body theory to avoid double counting of ladder contributions. The expansion for \tilde{V} can be found in e.g. Migdal [28], and to lowest order $\tilde{V} = V$, the free-space two-particle interaction. Higher order terms include contributions from e.g. density- and spin-density fluctuations. In this first exploratory calculation we will follow Ref. [27] and use the bare hyperon-hyperon interaction in Eq. (11). The relevant hyperon fractions and single-particle energies are taken from the BHF calculations described earlier in this paper. Details of the numerical solution of the gap equation can be found in Ref. [22].

Fig. 5 shows the energy gap $\Delta_F \equiv \Delta(k_F^{(\Sigma^-)})$ as a function of the total baryon density for Σ^- hyperons in β -stable matter for the NSC97E model. Although Λ may appear at higher densities, the 1S_0 Λ - Λ matrix elements of the NSC97E interaction are all repulsive, and therefore the energy gap for Λ hyperons would (to lowest order) have been zero at all densities, i.e. these particles would not have formed a superfluid. This is at variance with the results of Ref. [26], however, as remarked earlier this work employs an effective, parametrized interaction to drive the gap equation and therefore overestimates the Λ energy gap. Our Σ^- results are comparable to those of Ref. [27] which were obtained with a gaussian soft core parametrization of the bare Σ^- - Σ^- interaction.

If taken at face value these results have implications for neutron star cooling. Since at low densities Σ^- is the only hyperon species that is present in our calculation, the most important contribution to the neutrino cooling rate at such densities comes from the reaction $\Sigma^- \rightarrow n + e^- + \bar{\nu}_e$. According to Ref. [29] the threshold density for this reaction to occur is at around $2.4n_0$. If the Σ^- s are superfluid with energy gaps similar to what we found here, a sizeable reduction of the order of $\exp(-\Delta_F/kT)$ may be expected in the reaction rate. If neutron stars were to cool through direct Urca processes, their surface temperatures would be barely detectable within less than 100 yr of the star's birth. This is at askance with present observations. Thus, the formation of a hyperon superfluid will clearly suppress the hyperon direct Urca process and cooling will most likely proceed through less efficient processes and bring the results closer to experimental surface temperatures.

D. Structure of neutron stars

We end this section with a discussion on neutron star properties with the above equations of state.

The best determined neutron star masses are found in binary pulsars and all lie in the range $1.35 \pm 0.04 M_\odot$ [30] except for the nonrelativistic pulsar PSR J1012+5307 of mass $M = (2.1 \pm 0.8) M_\odot$ [31]. Several X-ray binary masses have been measured of which the heaviest are Vela X-1 with $M = (1.9 \pm 0.2) M_\odot$ [32] and Cygnus X-2 with $M = (1.8 \pm 0.4) M_\odot$ [33]. The recent discovery of high-frequency brightness oscillations in low-mass X-ray binaries provides a promising new method for determining masses and radii of neutron stars, see Ref. [34]. The kilohertz quasi-periodic oscillations (QPO) occur in pairs and are most likely the orbital frequencies of accreting matter in Keplerian orbits around neutron stars of mass M and its beat frequency with the neutron star spin. According to Zhang *et al.* [35] and Kaaret *et al.* [36] the accretion can for a few QPO's be tracked to its innermost stable orbit. For slowly rotating stars the resulting mass is $M \simeq 2.2 M_\odot (\text{kHz}/\nu_{QPO})$. For example, the maximum frequency of 1060 Hz upper QPO observed in 4U 1820-30 gives $M \simeq 2.25 M_\odot$ after

correcting for the neutron star rotation frequency. If the maximum QPO frequencies of 4U 1608-52 ($\nu_{QPO} = 1125$ Hz) and 4U 1636-536 ($\nu_{QPO} = 1228$ Hz) also correspond to innermost stable orbits the corresponding masses are $2.1M_{\odot}$ and $1.9M_{\odot}$. These constraints give us an upper limit for the mass of the order of $M \sim 2.2M_{\odot}$ and a lower limit $M \sim 1.35M_{\odot}$ and restrict thereby severely the EoS for dense matter.

In the following, we display the results for mass and radius using the equations of state discussed above. In order to obtain the radius and mass of a neutron star, we have solved the Tolman-Oppenheimer-Volkov equation with and without rotational corrections, following the approach of Hartle [37], see also Ref. [13]. Our results are shown in in Figs. 6 and 7. The equations of state we have used are those for

1. β -stable pn -matter with the parametrization of the results from Akmal *et al.* [11] made in Ref. [13]. This EoS is rather stiff compared with the EoS obtained with hyperons, see Fig. 3. The EoS yields a maximum mass $M \sim 1.9M_{\odot}$ without rotational corrections and $M \sim 2.1M_{\odot}$ when rotational corrections are included. The results for the mass are shown in Fig. 6 as functions of central density n_c . They are labelled as pn -matter with and without rotational corrections. The corresponding mass-radius relation (without rotational corrections) is shown in Fig. 7.
2. The other EoS employed is that which combines the nucleonic part of Ref. [11] with the computed hyperon contribution. As can be seen from Fig. 6, the softening of the EoS due to additional binding from hyperons leads to a reduction of the total mass. Without rotational corrections, we obtain a maximum mass $M \sim 1.3M_{\odot}$ whilst the rotational correction increases the mass to $M \sim 1.4M_{\odot}$. The size of the reduction, $\Delta M \sim 0.6 - 0.7M_{\odot}$, and the obtained neutron star masses due to hyperons are comparable to those reported by Balberg *et al.* [5].

There are other features as well to be noted from Fig. 6. The EoS with hyperons reaches a maximum mass at a central density $n_c \sim 1.2 - 1.3 \text{ fm}^{-3}$. In Fig. 2 we showed that the only hyperons which can appear at these densities are Λ and Σ^- . If other hyperons were

to appear at higher densities, this would most likely lead to a further softening of the EoS, and thereby smaller neutron star masses. Furthermore, the softer EoS yields also a smaller moment of inertia, as seen in Fig. 8.

The reader should however note that our calculation of hyperon degrees freedom is based on a non-relativistic Brueckner-Hartree-Fock approach. Although the nucleonic part extracted from Ref. [11], including three-body forces and relativistic boost corrections, is to be considered as a benchmark calculation for nucleonic degrees of freedom, relativistic effects in the hyperonic calculation could result in a stiffer EoS and thereby larger mass. However, relativistic mean field calculations with parameters which result in a similar composition of matter as shown in Fig. 2, result in similar masses as those reported in Fig. 6. In this sense, our results may provide a lower and upper bounds for the maximum mass. This leaves two natural options when compared to the observed neutron star masses. If the above heavy neutron stars prove erroneous by more detailed observations and only masses like those of binary pulsars are found, this may indicate that heavier neutron stars simply are not stable which in turn implies a soft EoS, or that a significant phase transition must occur already at a few times nuclear saturation densities. Our EoS with hyperons would fit into this case, although the mass without rotational corrections is on the lower side. Else, if the large masses from QPO's are confirmed, then the EoS for baryonic matter needs to be stiffer and in our case, this would rule out the presence of hyperons up to densities $\sim 10n_0 = 1.2 \text{ fm}^{-3}$.

Although we have only considered the formation of hyperons in neutron stars, transitions to other degrees of freedom such as quark matter, kaon condensation and pion condensation may or may not take place in neutron star matter. We would however like to emphasize that the hyperon formation mechanisms is perhaps the most robust one and is likely to occur in the interior of a neutron star, unless the hyperon self-energies are strongly repulsive due to repulsive hyperon-nucleon and hyperon-hyperon interactions, a repulsion which would contradict present data on hypernuclei [38]. The EoS with hyperons yields however neutron star masses without rotational corrections which are even below $\sim 1.4M_\odot$. This means that our EoS with hyperons needs to be stiffer, a fact which may in turn imply that more

complicated many-body terms not included in our calculations, such as three-body forces between nucleons and hyperons and/or relativistic effects, are needed.

III. CONCLUSIONS

Employing the recent parametrization of the free baryon-baryon potentials for the complete baryon octet of Stoks and Rijken [7], we have performed a microscopic many-body calculation of the structure of β -stable neutron star matter including hyperonic degrees of freedom. The potential model employed allows for the presence of only two types of hyperons up to densities ten times nuclear matter saturation density. These hyperons are Σ^- and Λ . The interactions for strangeness $S = -1$, $S = -2$, $S = -3$ and $S = -4$ are not attractive enough to allow the formation of other hyperons. The presence of hyperons leads however to a considerable softening of the EoS, entailing a corresponding reduction of the maximum mass of the neutron star. With hyperons, we obtain maximum masses of the order $M \sim 1.3 - 1.4M_\odot$.

In addition, since Σ^- hyperons appear already at total baryonic densities $\sim n = 0.27 \text{ fm}^{-3}$), we have also considered the possibility of forming a hyperon superfluid. The latter would in turn quench the increased emission of neutrinos due to the presence of hyperons. Within our many-body approach, we find that Σ^- forms a superfluid in the 1S_0 wave, whereas the $\Lambda - \Lambda$ interaction for the same partial wave leads to a vanishing gap for the potential model employed here.

We are much indebted to H. Heiselberg, H.-J. Schulze and V. G. J. Stoks for many useful comments. This work has been supported by the DGICYT (Spain) Grant PB95-1249 and the Program SCR98-11 from the Generalitat de Catalunya. One of the authors (I.V.) wishes to acknowledge support from a doctoral fellowship of the Ministerio de Educación y Cultura (Spain).

REFERENCES

- [1] M. Prakash, I. Bombaci, M. Prakash, P. J. Ellis, J.M. Lattimer, and R. Knorren, Phys. Rep. **280**, 1 (1997).
- [2] R. Knorren, M. Prakash and P. J. Ellis, Phys. Rev. C **52**, 3470 (1995).
- [3] J. Schaffner and I. Mishustin, Phys. Rev. C **53**, 1416 (1996).
- [4] S. Balberg and A. Gal, Nucl. Phys. **A625**, 435 (1997).
- [5] S. Balberg, I. Lichtenstadt, and G. B. Cook, Ap. J. Suppl. **121**, 515 (1999).
- [6] H.-J. Schulze, M. Baldo, U. Lombardo, J. Cugnon, and A. Lejeune, Phys. Rev. C **57**, 704 (1998); M. Baldo, G.F. Burgio, and H.-J. Schulze, Phys. Rev. C **58**, 3688 (1998).
- [7] V. G. J. Stoks and Th. A. Rijken, Phys. Rev. C **59**, 3009 (1999).
- [8] I. Vidaña, A. Polls, A. Ramos, M. Hjorth-Jensen, and V. G. J. Stoks, preprint nucl-th/9909019 and Phys. Rev. C, in press.
- [9] Th. A. Rijken, V. G. J. Stoks, and Y. Yamamoto, Phys. Rev. C **59**, 21 (1998).
- [10] V. G. J. Stoks and T.-S. H. Lee, Phys. Rev. C **60**, 024006 (1999).
- [11] A. Akmal, V. R. Pandharipande, and D. G. Ravenhall, Phys. Rev. C **58**, 1804 (1998).
- [12] R. B. Wiringa, V. G. J. Stoks, and R. Schiavilla, Phys. Rev. C **51**, 38 (1995).
- [13] H. Heiselberg and M. Hjorth-Jensen, Phys. Rep., in press and nucl-th/9902033; Ap. J., **525**, L41 (1999).
- [14] I. Vidaña, A. Polls, A. Ramos, and M. Hjorth-Jensen, (unpublished).
- [15] I. Vidaña, A. Polls, A. Ramos, and M. Hjorth-Jensen, Nucl. Phys. **A644**, 201 (1998).
- [16] C. J. Batty, E. Friedman, and A. Gal, Phys. Rev. C **59**, 295 (1999).
- [17] M. Baldo, J. Cugnon, A. Lejeune, and U. Lombardo, Nucl. Phys. A **515**, 409 (1990).

- [18] M. Baldo, J. Cugnon, A. Leujeune, and U. Lombardo, Nucl. Phys. A **536**, 349 (1992).
- [19] J. Wambach, T. L. Ainsworth, and D. Pines, Nucl. Phys. A **555**, 128 (1993).
- [20] H.-J. Schulze, J. Cugnon, A. Leujeune, M. Baldo, and U. Lombardo, Phys. Lett. B **375**, 1 (1996).
- [21] V. A. Khodel, V. V. Khodel, and J. W. Clark, Nucl. Phys. A **598**, 390 (1996).
- [22] Ø. Elgarøy, L. Engvik, M. Hjorth-Jensen, and E. Osnes, Nucl. Phys. A **604**, 466 (1996).
- [23] M. Baldo, Ø. Elgarøy, L. Engvik, M. Hjorth-Jensen, and H.-J. Schulze, Phys. Rev. C **58**, 1921 (1998).
- [24] P. W. Anderson and N. Itoh, Nature **256**, 25 (1975).
- [25] Ø. Elgarøy, L. Engvik, E. Osnes, F. V. De Blasio, M. Hjorth-Jensen, and G. Lazzari, Phys. Rev. Lett. **76**, 1994 (1996).
- [26] S. Balberg and N. Barnea, Phys.Rev. C **57**, 409 (1998).
- [27] T. Takatsuka and R. Tamagaki, to be published in Proceedings from APCTP Workshop on “Strangeness Nuclear Physics”.
- [28] A. B. Migdal, *Theory of Finite Fermi Systems and Applications to Atomic Nuclei*, (Wiley, New York, 1967).
- [29] C. Schaab, S. Balberg, and J. Schaffner-Bielich, Ap. J. **504**, L99 (1998).
- [30] S. E. Thorsett and D. Chakrabarty, Ap. J. **512**, 288 (1999).
- [31] J. van Paradijs, astro-ph/9802177 and in: The Many Faces of Neutron Stars, Eds. R. Buccheri, J. van Paradijs and M.A. Alpar, (Kluwer, Dordrecht, 1999) in press
- [32] S. Barziv *et al.*, (unpublished).
- [33] J.A. Orosz and E. Kuulkers, Mon. Not. R. Astron. Soc., in press and astro-ph/9901177.

- [34] M. C. Miller, F. K. Lamb, , and P. Psaltis, *Ap. J.* **508**, 791 (1998).
- [35] W. Zhang, T. E. Strohmayer, and J. H. Swank, *Ap. J.* **482**, L167 (1997); W. Zhang, A. P. Smale, T. E. Strohmayer, and J. H. Swank, *Ap. J.* **500**, L171 (1998).
- [36] P. Kaaret, E. C. Ford, and K. Chen, *Ap. J.* **480**, L27 (1997).
- [37] J. B. Hartle, *Ap. J.* **150**, 1005 (1967).
- [38] H. Bandō, T. Motoba, and J. Žofka, *Int. J. Mod. Phys.* **A5**, 4021 (1990).

FIGURES

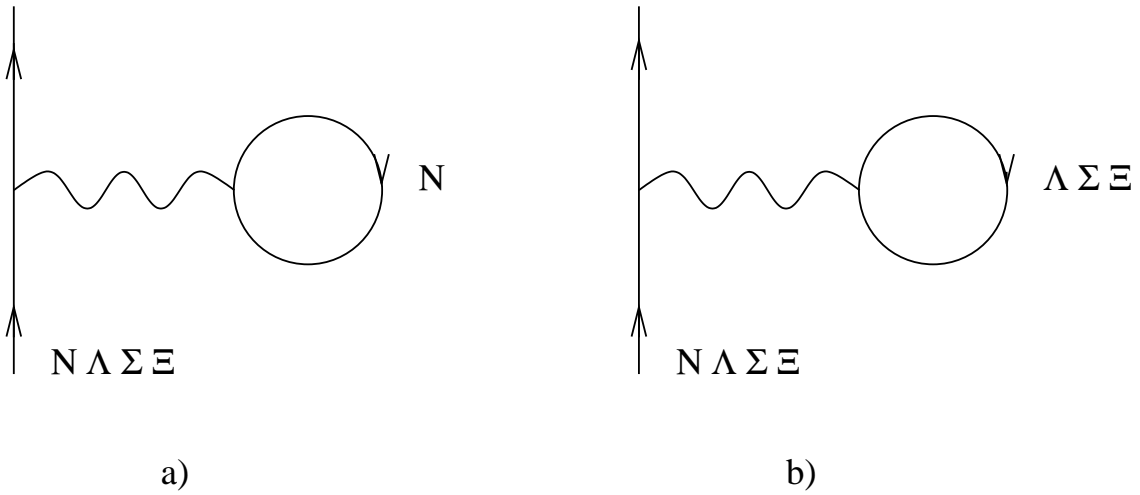


FIG. 1. Goldstone diagrams for the single-particle potential u . a) represents the contribution from nucleons only as hole states while b) includes only hyperons as hole states. The wavy line represents the G -matrix.

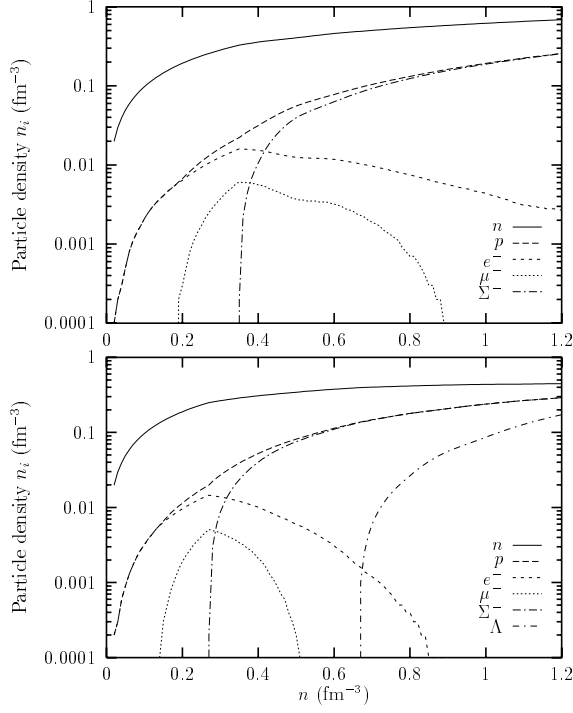


FIG. 2. Particle densities in β -stable neutron star matter as functions of the total baryonic density n . The upper panel represents the results obtained at the Brueckner-Hartree-Fock level with the potential of Stoks and Rijken [7]. In the lower panel the nucleonic part of the self-energy of the nucleons has been replaced with the EoS of Ref. [11]. For the latter, (not shown in the figure) positrons appear at a density 1.18 fm^{-3} .

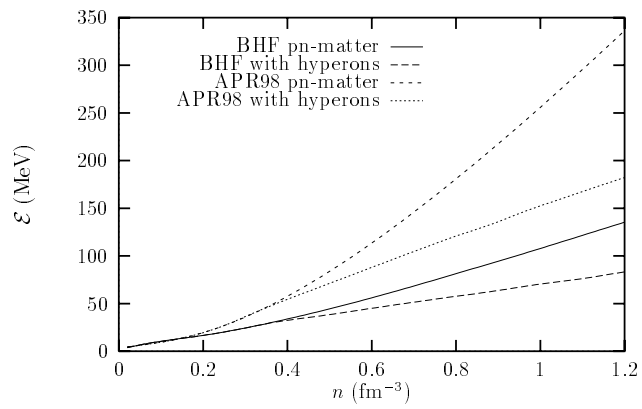


FIG. 3. Energy per baryon in β -stable neutron star matter for different approaches as function of the total baryonic density n . See text for further details.

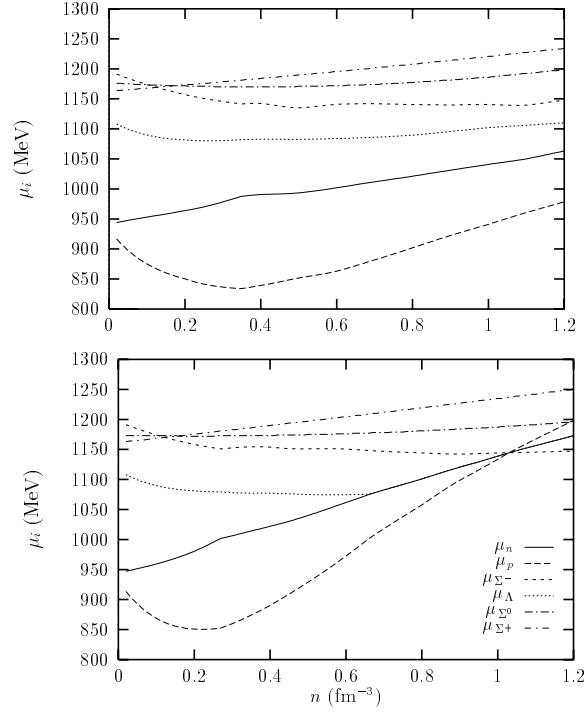


FIG. 4. Chemical potentials in β -stable neutron star matter as functions of the total baryonic density n . The upper panel represents the results obtained at the Brueckner-Hartree-Fock level with the potential of Stoks and Rijken [7]. The lower panel includes results obtained with the EoS of Ref. [11].

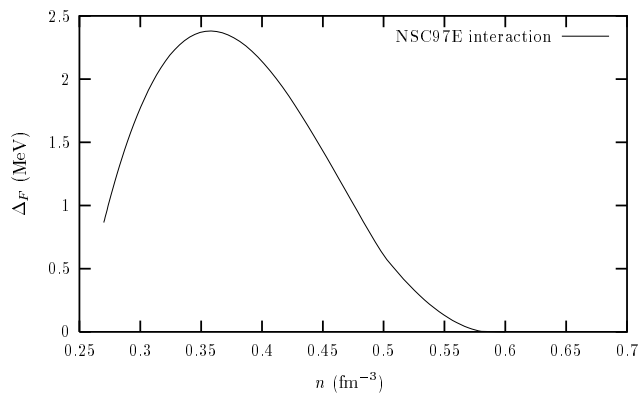


FIG. 5. Energy gap Δ_F as a function of the total baryon density for Σ^- hyperons in β -stable matter.

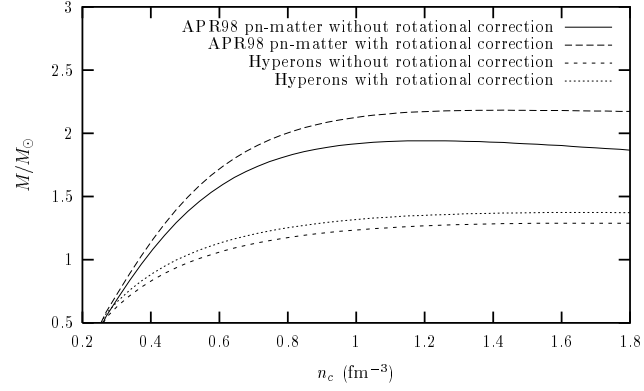


FIG. 6. Total mass M for various equations of state. See text for further details.

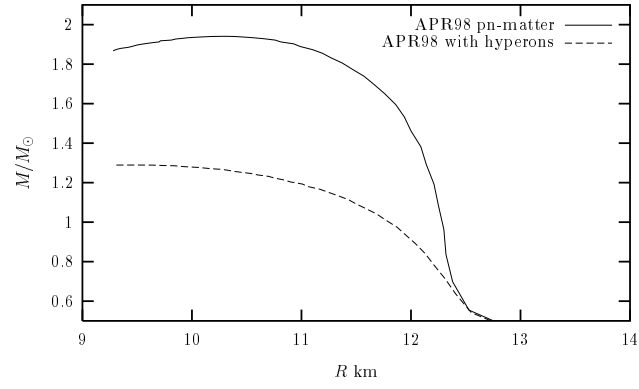


FIG. 7. Mass-radius relation without rotational corrections for various various equations of state.

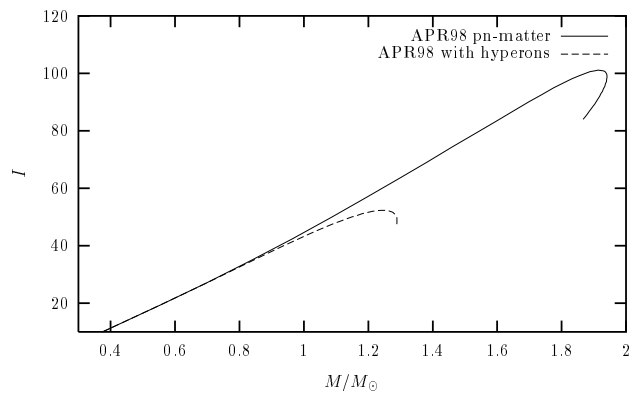


FIG. 8. The maximum moment of Inertia I , in units of $M_{\odot}\text{km}^2$. Same equations of state as in the preceding figure. All results are for β -stable matter and rotational corrections have not been included in the total mass.